Supporting information

A heterometallic sodium(I)-europium(III)-organic layer exhibiting dual-responsive luminescent sensing for nitrofuran antibiotics, $Cr_2O_7^{2-}$ and MnO_4^- anions

Shan Xu,[a] Jing-Jing Shi,[a] Bo Ding,[a] Zheng-Yu Liu,[a] Xiu-Guang Wang,[a] Xiao-Jun Zhao*[a, b] and En-Cui Yang*[a]

Table S1 Selected bond lengths (Å) and angles (deg) for **1** [a]

Eu(1)–O(1)	2.441(5)	Eu(2)–O(10)	2.374(5)
Eu(1)–O(2)	2.467(5)	Eu(2)–O(11)$^{\#1}$	2.511(4)
Eu(1)–O(5)	2.473(5)	Eu(2)–O(12)$^{\#1}$	2.437(5)
Eu(1)–O(6)	2.523(4)	Eu(2)–O(14)	2.431(5)
Eu(1)–O(8)$^{\#1}$	2.392(5)	Eu(2)–O(16)	2.312(5)
Eu(1)–O(9)	2.315(5)	Na(1)–O(2)	2.506(5)
Eu(1)–O(13)	2.341(6)	Na(1)–O(4)$^{\#}$5	2.371(5)
Eu(1)–O(15)	2.422(5)	Na(1)–O(6)	2.292(6)
Eu(2)–O(3)$^{\#3}$	2.463(5)	Na(1)–O(11)$^{\#2}$	2.285(6)
Eu(2)–O(4)$^{\#3}$	2.453(5)	Na(1)–O(14)$^{\#4}$	2.546(6)
Eu(2)–O(7)$^{\#1}$	2.280(5)	Na(1)–O(15)	2.406(5)
O(1)–Eu(1)–O(2)	52.66(15)	O(7)$^{\#1}$–Eu(2)–O(12)$^{\#1}$	81.8(2)
O(1)–Eu(1)–O(5)	79.45(19)	O(7)$^{\#1}$–Eu(2)–O(14)	80.47(19)
O(1)–Eu(1)–O(6)	102.53(17)	O(7)$^{\#1}$–Eu(2)–O(16)	110.70(18)
O(2)–Eu(1)–O(5)	92.22(18)	O(10)–Eu(2)–O(3)$^{\#2}$	79.99(18)
O(2)–Eu(1)–O(6)	71.35(17)	O(10)–Eu(2)–O(4)$^{\#2}$	132.04(17)
O(5)–Eu(1)–O(6)	51.73(16)	O(10)–Eu(2)–O(11)$^{\#1}$	129.42(17)

O(8)$^{\#1}$–Eu(1)–O(1)	81.75(17)	O(10)–Eu(2)–O(12)$^{\#1}$	78.55(17)
O(8)$^{\#1}$–Eu(1)–O(2)	134.31(17)	O(10)–Eu(2)–O(14)	149.13(17)
O(8)$^{\#1}$–Eu(1)–O(5)	80.88(17)	O(12)$^{\#1}$–Eu(2)–O(3)$^{\#2}$	78.93(19)
O(8)$^{\#}$1–Eu(1)–O(6)	129.54(17)	O(12)$^{\#1}$–Eu(2)–O(4)$^{\#2}$	96.22(19)
O(8)$^{\#1}$–Eu(1)–O(15)	147.05(16)	O(12)$^{\#1}$–Eu(2)–O(11)$^{\#1}$	52.00(16)
O(13)–Eu(1)–O(6)	148.25(18)	O(14)–Eu(2)–O(3)$^{\#2}$	122.30(18)
O(9)–Eu(1)–O(2)	141.91(16)	O(14)–Eu(2)–O(4)$^{\#2}$	71.41(16)
O(9)–Eu(1)–O(5)	84.55(19)	O(14)–Eu(2)–O(11)$^{\#1}$	72.53(17)
O(9)–Eu(1)–O(6)	77.17(16)	O(14)–Eu(2)–O(12)$^{\#1}$	123.65(17)
O(9)–Eu(1)–O(8)$^{\#1}$	82.72(18)	O(16)–Eu(2)–O(3)$^{\#2}$	82.10(18)
O(9)–Eu(1)–O(13)	107.29(19)	O(16)–Eu(2)–O(4)$^{\#2}$	86.36(18)
O(9)–Eu(1)–O(15)	79.45(18)	O(16)–Eu(2)–O(10)	80.37(19)
O(13)–Eu(1)–O(1)	84.07(19)	O(16)–Eu(2)–O(11)$^{\#1}$	149.97(18)
O(13)–Eu(1)–O(2)	89.63(19)	O(16)–Eu(2)–O(14)	82.02(18)
O(13)–Eu(1)–O(8)$^{\#1}$	81.94(19)	O(4)$^{\#5}$–Na(1)–O(2)	105.04(18)
O(13)–Eu(1)–O(15)	77.28(18)	O(4)–Na(1)–O(14)$^{\#4}$	70.75(17)
O(15)–Eu(1)–O(1)	120.62(17)	O(15)–Na(1)–O(14)$^{\#4}$	113.59(19)
O(15)–Eu(1)–O(2)	71.20(16)	O(6)–Na(1)–O(2)	74.53(19)
O(15)–Eu(1)–O(5)	124.26(16)	O(6)–Na(1)–O(4)$^{\#5}$	100.1(2)
O(15)–Eu(1)–O(6)	72.65(16)	O(6)–Na(1)–O(14)$^{\#4}$	111.1(2)
O(3)$^{\#2}$–Eu(2)–O(11)$^{\#1}$	98.02(17)	O(6)–Na(1)–O(15)	77.15(18)
O(4)$^{\#}$2–Eu(2)–O(3)$^{\#2}$	52.50(16)	O(11)$^{\#3}$–Na(1)–O(4)$^{\#5}$	76.26(19)
O(4)$^{\#2}$–Eu(2)–O(11)$^{\#1}$	70.79(17)	O(11)$^{\#3}$–Na(1)–O(14)$^{\#4}$	74.26(18)
O(7)$^{\#1}$–Eu(2)–O(4) $^{\#2}$	144.78(17)	O(11)$^{\#3}$–Na(1)–O(15)	106.0(2)

O(7)$^{\#1}$–Eu(2)–O(10)	82.32(19)	O(15)–Na(1)–O(2)	70.79(17)
O(7)$^{\#1}$–Eu(2)–O(11)$^{\#1}$	80.97(16)		

[a] Symmetry codes: $^{\#1}$ $x, y + 1, z$; $^{\#2}$ $x - 1, 3/2 - y, z - 1/2$; $^{\#3}$ $-x, y + 1/2, 3/2 - z$; $^{\#4}$ $-x, y - 1/2, 3/2 - z$; $^{\#5}$ $1 - x, 1 - y, 2 - z$; $^{\#6}$ $1 + x, 3/2 - y, z + 1/2$; $^{\#7}$ $x, y - 1, z$.

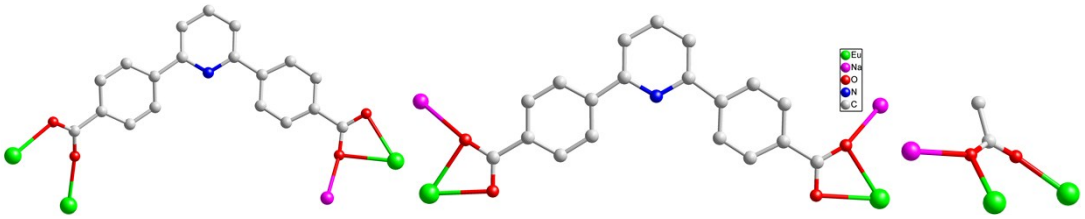

μ_4-η^1:η^2:η^1:η^1 μ_4-η^2:η^1:η^1:η^2 μ_3-η^1:η^2

Fig. S1 Binding modes of $pddb^{2-}$ and acetate anion.

Table S2 Hydrogen-boding parameters (Å, deg) in **1** [a]

D–H···A	*d* (D–H)	*d* (H···A)	*d* (D···A)	∠(D–H···A)
C28–H28···O1	0.93	2.56	3.209	128
C48–H48···O3	0.93	2.41	3.304	162

[a] Symmetry codes: [#1] $-x$, $1-y$, $2-z$.

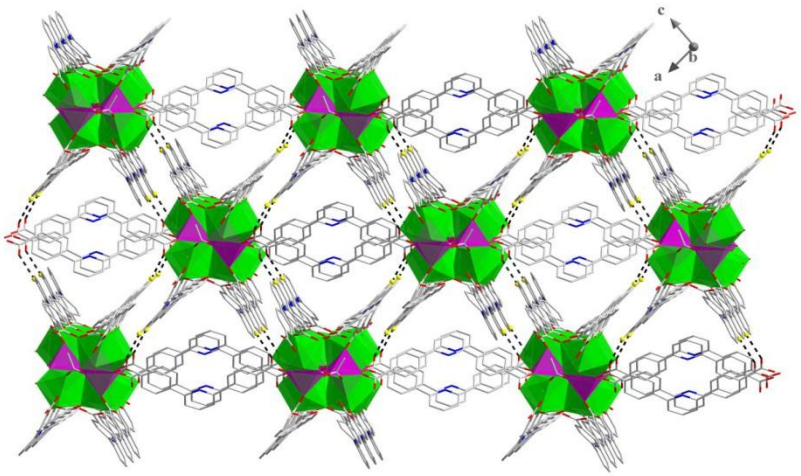

Fig. S2 3D supramolecular framework of **1**.

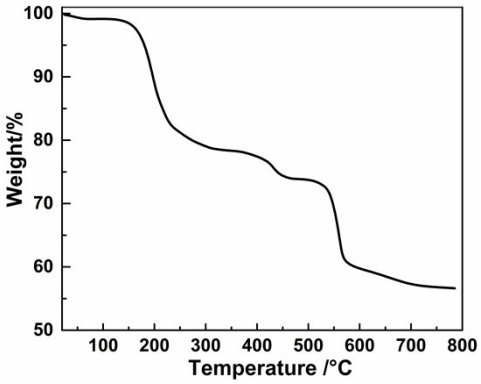

Fig. S3 TGA curve of **1**.

Table S3 Fluorescence lifetime of **1** in the solid state and dispersed in DMF in the absence and presence of NFZ, NFT and $Cr_2O_7^{2-}$

Sample	τ_1 (μs)	%	τ_2 (μs)	%	Lifetime (μs)
1	317	2.19	971	97.81	1018.78
1-DMF suspension	87	2.77	959	97.23	956.36
1 + NFZ (0.13 mM)	95	2.46	958	97.56	958.07
1 + NFT (0.13 mM)	85	2.07	954	97.93	951.56
1 + FZD (0.13 mM)	94	2.26	951	97.74	950.51
1 + $Cr_2O_7^{2-}$ (0.67 mM)	109	2.73	955	97.27	958.71
1 + MnO_4^- (0.67 mM)	89	1.68	955	98.32	953.71

Table S4 Standard deviation (σ) calculated from the five blank measurements.

Blank Readings	NFZ	NFT	FDZ	$Cr_2O_7^{2-}$	MnO_4^-
#1 Fluorescence Intensity (CPS)	1114385	1114385	1114385	1056255	1056255
#2 Fluorescence Intensity (CPS)	1110000	1110000	1110000	1067350	1067350
#3 Fluorescence Intensity (CPS)	1111070	1111070	1111070	1057650	1057650
#4 Fluorescence Intensity (CPS)	1108240	1108240	1108240	1055530	1055530
#5 Fluorescence Intensity (CPS)	1093660	1093660	1093660	1048050	1048050
Standard Deviation (σ)	8038.767	8038.767	8038.767	6898.514	6898.514

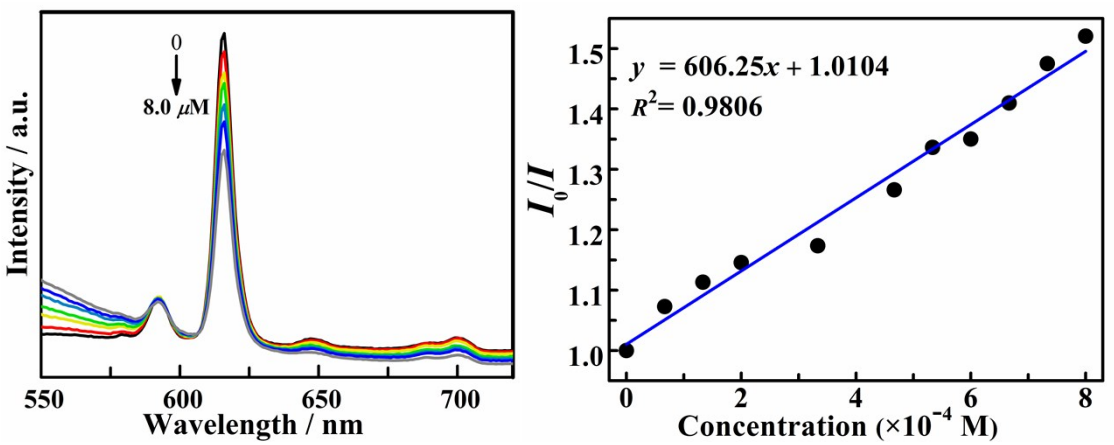

(a) (b)

Fig. S4 (a) Fluorescence spectra of **1** upon incremental addition of $Cr_2O_7^{2-}$ in alkaline DMF solution. (b) Plot of I_0/I vs. $[Cr_2O_7^{2-}]$ in alkaline DMF solution (The blue solid lines represent the linear fit to the Stern−Volmer equation).

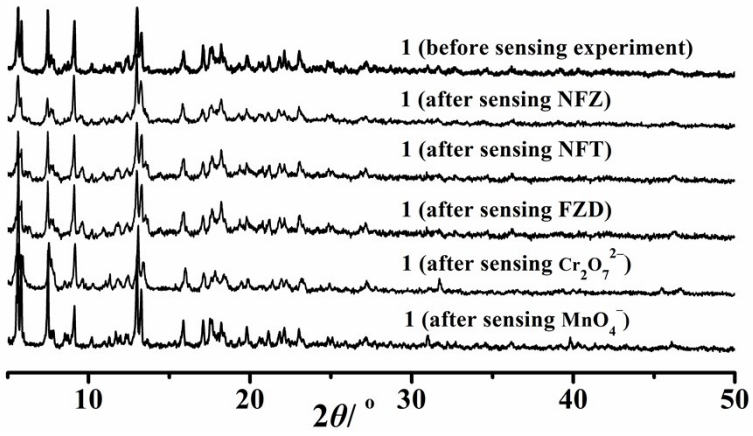

Fig. S5 PXRD patterns of **1** before after detecting of NFs, $Cr_2O_7^{2-}$ and MnO_4^-.

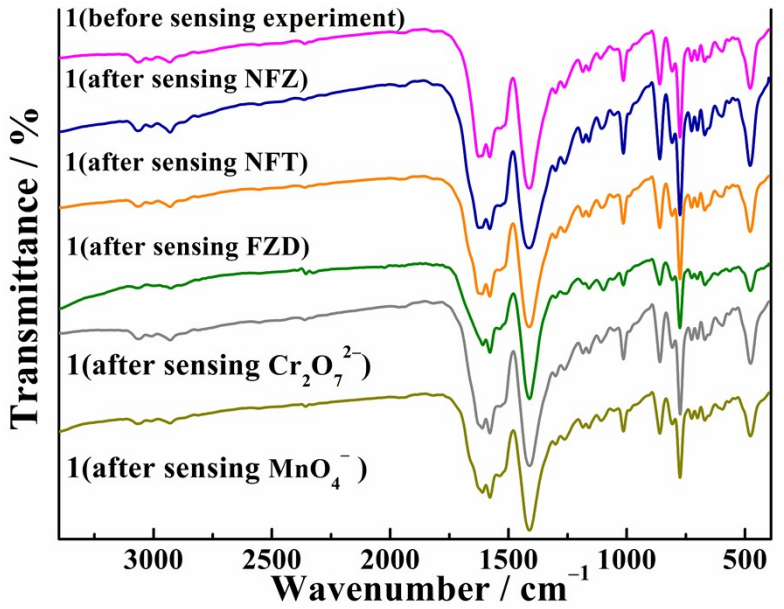

Fig. S6 FT-IR spectra of **1** before and after the detection of NFs, $Cr_2O_7^{2-}$ and MnO_4^-.